RESOLUTION AND INCOHERENT COMBINATION OF MULTIPATH ARRIVALS

Albert H. Nuttall

Naval Underwater Systems Center
Newport, Rhode Island

17 January 1973

NUSC Technical Report 4481

Resolution and Incoherent Combination Of Multipath Arrivals

ALBERT H. NUTTALL
Office of the Director
of Science and Technology

17 January 1973

NAVAL UNDERWATER SYSTEMS CENTER

32

JJW to NUSC Ltr. LA152-119

ADMINISTRATIVE INFORMATION

This study was performed under NUSC Project No. A-752-05, "Statistical Communication with Applications to Sonar Signal Processing," Principal Investigator, Dr. A. H. Nuttall (Code TC) and Navy Subproject and Task No. ZF 61 112 001, Program Manager, Dr. J. H. Huth (CNM Code MAT 03L4). Also, this report was prepared under NUSC Project No. A-686-01, "Project SUBSACS," Principal Investigator, Dr. D. W. Hyde (Code TC).

The Technical Reviewer for this report was Dr. D. W. Hyde.

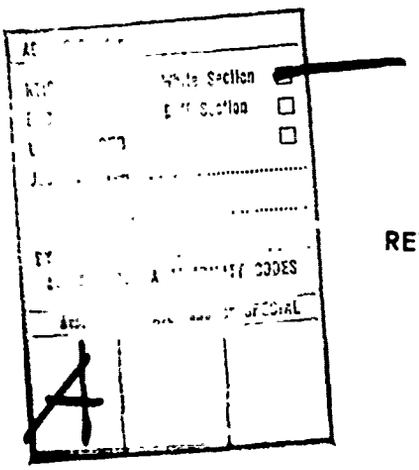

REVIEWED AND APPROVED: 17 January 1973

W. A. Von Winkle
Director of Science and Technology

Inquiries concerning this report may be addressed to the author,
New London Laboratory, Naval Underwater Systems Center,
New London, Connecticut 06320

UNCLASSIFIED
Security Classification

DOCUMENT CONTROL DATA - R & D

Security classification of title, body of abstract and indexing annotation must be entered when the overall report is classified)

1 ORIGINATING ACTIVITY (Corporate author) NUSC Newport, Rhode Island 02840	2a. REPORT SECURITY CLASSIFICATION UNCLASSIFIED 2b. GROUP

3 REPORT TITLE

RESOLUTION AND INCOHERENT COMBINATION OF MULTIPATH ARRIVALS

4 DESCRIPTIVE NOTES (Type of report and inclusive dates)
Research Report

5 AUTHOR(S) (First name, middle initial, last name)
Albert H. Nuttall

6 REPORT DATE 17 January 1973	7a. TOTAL NO. OF PAGES 36	7b. NO. OF REFS 2
8a CONTRACT OR GRANT NO b. PROJECT NO A-752-05 c. ZF 61 112 001 d.	9a. ORIGINATOR'S REPORT NUMBER(S) TR 4481 9b. OTHER REPORT NO(S) (Any other numbers that may be assigned this report)	

10 DISTRIBUTION STATEMENT
Approved for public release; distribution unlimited

11 SUPPLEMENTARY NOTES	12 SPONSORING MILITARY ACTIVITY Department of the Navy

13 ABSTRACT

The performance capability associated with resolving and incoherently combining multipath arrivals is investigated, as a function of the signaling bandwidth, for a generic communications system. The performance measure used is a deflection criterion of receiver output signal-to-noise ratio. It is shown that resolution and incoherent combination is a form of diversity which yields a measure of safety, in that drastic losses in performance become far less likely. The exact behavior of the signal-to-noise ratio depends on the detailed medium impulse response; several examples are investigated.

1a

DD FORM 1 NOV 68 1473 (PAGE 1)
S/N 0102-014-6600

UNCLASSIFIED
Security Classification

14 KEY WORDS	LINK A		LINK B		LINK C	
	ROLE	WT	ROLE	WT	ROLE	WT
Multipath Resolution						
Incoherent Combination						
Performance Capability						
Signal Bandwidth Dependence						
Deflection Criterion						
Medium Impulse Response						

Ib

TABLE OF CONTENTS

LIST OF ILLUSTRATIONS

REVERSE BLANK

LIST OF SYMBOLS

t	Time
$x(t)$	Transmitted signal (complex envelope)
f	Frequency
f_o	Carrier frequency
T	Transmitted signal duration
W	Transmitted signal bandwidth
E_x	Transmitted signal energy
τ	Delay variable
$h_m(\tau)$	Medium impulse response (complex envelope)
L	Medium impulse duration
W_m	Medium bandwidth
B	Medium frequency spread
$n(t)$	Additive noise (complex envelope)
N_d	Noise spectrum level (double-sided)
$y(t)$	Received process (complex envelope)
$h_r(\tau)$	Receiver processing filter impulse response (complex envelope)
$H_r(f)$	Receiver processing filter transfer function
$z(t)$	Receiver filter output (complex envelope)
$e(t)$	Detector output
$h_a(\tau)$	Averaging-filter impulse response
L_a	Averaging-filter duration
$r(t)$	System output
$d_e(t)$, $d_r(t)$	Deflection criteria
A_k	Area of k-th component pulse in the medium impulse response
N	Measure of the number of pulses in the medium impulse response
d_{e_2}	Maximum possible deflection of the optimum receiver

LIST OF SYMBOLS (Cont'd)

$\phi(t)$	Autocorrelation of $x(t)$
$p(t)$	Approximation to $\phi(t)$
$G_n(f)$	Power density spectrum of process $n(t)$
SNR	Signal-to-noise ratio
τ_d	Medium path delay difference
$U(f)$	Unit step function: 1 for $f > 0$, 0 for $f < 0$.
Re	Real part
E	Average value
Var	Variance
SD	Standard deviation
$\tilde{x}(t)$	Real waveform corresponding to $x(t)$
subscript s	Signal alone
subscript n	Noise alone
$\circledast$	Convolution
*	Complex conjugate
Overbar	Ensemble average

RESOLUTION AND INCOHERENT COMBINATION OF MULTIPATH ARRIVALS

INTRODUCTION

The time-varying impulse response of the ocean medium between transmitting and receiving points is often composed of several paths of varying strengths and relative delays. If a narrowband signal is transmitted through such a medium, the signal may encounter a deep fade and, thereby, seriously degrade communication performance. On the other hand, if a broadband signal is transmitted, the multipaths may be resolved at the output of a receiver matched filter, yielding a sequence of sharp pulses of varying strengths and relative delays. Incoherent combination of above-threshold pulses may improve the system detection and communication capability, without the receiver having to know the precise structure of the current medium impulse response. Here we investigate the system performance capability measured by a deflection criterion of receiver output signal-to-noise ratio, for large signal time-bandwidth products, as a function of signaling bandwidth and a very general model of the medium impulse response.

PROBLEM DEFINITION

A block diagram of the system to be considered is given in figure 1. The transmitted signal* $\mathrm{Re}\{x(t)\ \exp(i2\pi f_0 t)\}$ is a broadband signal centered on a carrier frequency. Its duration is T seconds and its bandwidth is W hertz; the signal time-bandwidth product TW is assumed to be much larger than unity. For example, x(t) may be a pseudorandom sequence. The energy of the <u>real</u> transmitted signal is E_x.

The medium impulse response $h_m(\tau)$ is of duration L, and the medium transfer function has bandwidth W_m. Thus significant changes in $h_m(\tau)$ can occur no faster than every $1/W_m$ seconds; they may occur much slower. The medium impulse response is very slowly time-varying; that is, medium frequency spread B satisfies the inequality $B^{-1} > T$. There is assumed to be no Doppler shift between transmitter and receiver. The detailed multipath structure of the medium is not known to the receiver. However, signal duration T is assumed to be much larger than multipath spread L.

---

*Complex notation is employed in the linear portion of the system in figure 1; see appendix A in reference 1, for example. Also, all functions are centered at the origin, for convenience, without loss of generality.

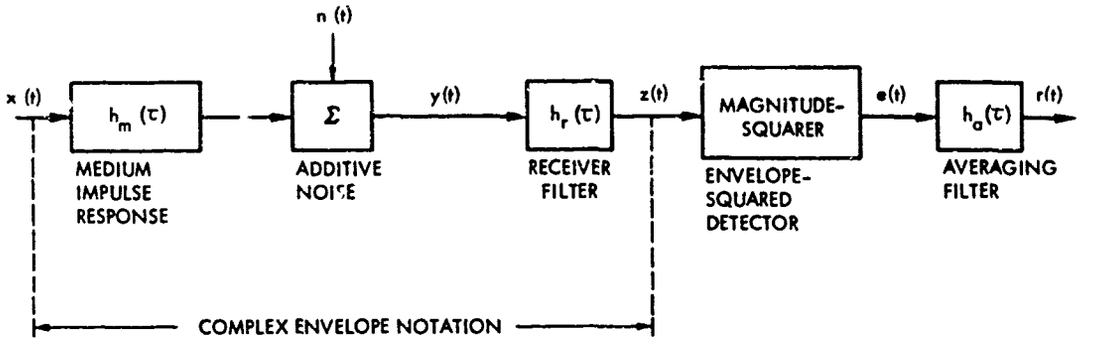

Figure 1. System Block Diagram

We assume that the additive noise n(t) is stationary Gaussian and white over the passband of the receiver filter $h_r(\tau)$. The noise (double-sided) spectrum level is N_d watts/hertz.

The receiver processing filter $h_r(\tau)$ is selected as the matched filter to transmitted signal x(t); i.e.,

$$h_r(\tau) = x^*(-\tau) , \tag{1}$$

$$H_r(f) = X^*(f) . \tag{2}$$

The envelope-squared detector is characterized mathematically by

$$e(t) = |z(t)|^2 , \tag{3}$$

since z(t) is a complex envelope, whereas e(t) is a real low-pass waveform.

Averaging filter $h_a(\tau)$ has an impulse response duration L_a, which should approximately equal the medium multipath duration L. Several choices are available for $h_a(\tau)$. If it is a simple unimodal function, the averaging filter merely adds up all resolved multipath signal outputs from the detector, in addition to the noisy intervals. If $h_a(\tau)$ were chosen instead to be a set of impulses of different areas and delays, the averaging filter would sample the detector output at several relative time delays, weight them, and add them. If the averaging-filter delays correspond to the actual medium path delays, then a near-optimum incoherent combination of multipath arrivals would take place. A practical approximation to this processor (which does not require knowledge of the medium path delays) is achieved by subjecting the detected output e(t) to a threshold and passing only those values above the threshold to the averaging filter. However, if any noise pulses exceed the threshold, they too would be

accumulated. Here we shall analyze only the performance of the simple unimodal averaging filter without thresholding. Later we shall comment on the performance of the thresholding technique.

For a given medium (L, W_m, detailed multipath), a given signal (T, E_x), and a given receiver (matched filter), we wish to investigate the performance capability of the system in figure 1, as a function of the signal bandwidth W. Should W be chosen larger or smaller than 1/L, and by how much? What are the trade-offs of the various choices, such as the increased noise allowed through the matched filter for larger W, and the effect of resolving individual multipath arrivals when $W > 1/L$ (i.e., $1/W < L$)? How much of the medium bandwidth W_m should be used? (There is no point in transmitting a signal of bandwidth greater than W_m, and, in fact, W may have to be chosen much smaller than W_m to avoid interference with other nearby transmitters and receivers.) It should be noted that since receiver processing filter $h_r(\tau)$ is matched to transmitted signal x(t), the receiver also changes with W, in addition to the transmitted signal changing.

A plot of a typical detector output waveform e(t) is depicted in figure 2, for $W > 1/L$. The central region of extent L is the important region for signal detection. In this region, the standard deviation of the output noise is the

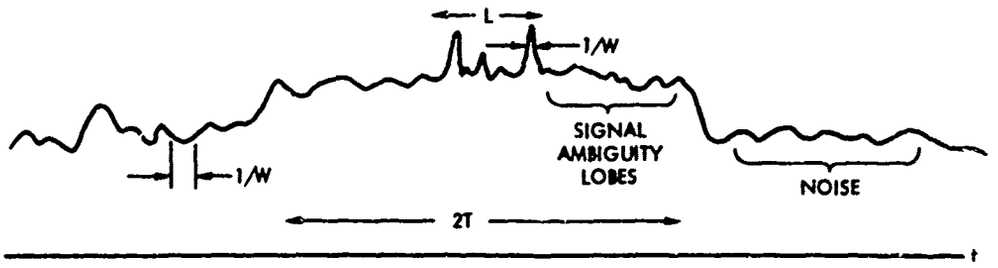

Figure 2. Detector Output Waveform

limiting factor. (The mean of the noise output raises the average output but does not limit detectability.) Accordingly, the performance measure adopted at the detector output for the system of figure 1 is the deflection criterion

$$d_e(t) \equiv \frac{e_s(t)}{SD\{e_n(t)\}}, \qquad (4)$$

where subscripts s and n denote signal alone and noise alone, respectively, and SD denotes standard deviation. Equation (4) is a function of time and can have several peaks if the medium multipath is resolved ($W > 1/L$); see figure 2.

The corresponding performance measure at the averaging filter output is

$$d_r(t) \equiv \frac{r_s(t)}{SD\ \{r_n(t)\}} . \qquad (5)$$

Both (4) and (5) are of interest here and will be investigated for several multipath profiles.

RESULTS

The derivations of (4) and (5) are presented in appendix A, and are available generally from (A-6), (A-7), (A-16), and (A-17). We now specialize these general results to particular cases. A very general model for the medium impulse response $h_m(\tau)$ is afforded by a sum of spaced complex Gaussian pulses:

$$h_m(\tau) = W_m \sum_{k=-N}^{N} A_k \exp\left[-\pi (W_m \tau - \frac{3}{4} k)^2\right] . \qquad (6)$$

The area of each pulse is A_k and is a measure of the voltage attenuation of a component path. By proper choice of N and $\{A_k\}$, a wide variety of impulse responses can be realized. The derivations of (4) and (5) for the model of (6) are presented in appendix A, along with some simplifying assumptions made for mathematical tractability. Equation (4) is given by

$$d_e(t) = \frac{E_x}{8N_d} \frac{1}{1 + \frac{W^2}{W_m^2}} \left| \sum_{k=-N}^{N} A_k \exp\left[-\pi \frac{\left(Wt - \frac{3}{4} k \frac{W}{W_m}\right)^2}{1 + \frac{W^2}{W_m^2}} \right] \right|^2 , \qquad (7)$$

while (5) becomes

$$d_r(t) = \frac{E_x}{8N_d} \left[\frac{\sqrt{1 + 4L_a^2 W_m^2 \frac{W^2}{W_m^2}}}{\left[1 + \frac{W^2}{W_m^2}\right] \left[1 + \frac{W^2}{W_m^2} (1 + 2L_a^2 W_m^2)\right]} \right]^{\frac{1}{2}} \times$$

$$\sum_{k,\ell=-N}^{N} A_k A_\ell^* \exp\left[-\frac{9}{32}\pi\frac{\frac{W^2}{W_m^2}}{1+\frac{W^2}{W_m^2}}(k-\ell)^2\right]\exp\left[-2\pi\frac{\left(Wt-\frac{3}{8}(k+\ell)\frac{W}{W_m}\right)^2}{1+\frac{W^2}{W_m^2}\left(1+2L_a^2W_m^2\right)}\right] \tag{8}$$

The fundamental dimensionless parameters are N, $\{A_k\}_{-N}^{N}$, LW, and L_a/L. All other parameters depend on these:

$$LW_m = 1 + \frac{3}{2}N \quad \text{(from (6))},$$

$$L_aW_m = \frac{L_a}{L}LW_m = \frac{L_a}{L}\left(1+\frac{3}{2}N\right), \quad \text{and}$$

$$\frac{W}{W_m} = \frac{LW}{LW_m} = \frac{LW}{1+\frac{3}{2}N}. \tag{9}$$

Signal duration T and detailed waveform do not appear in (7) or (8), because of the approximation made to the signal autocorrelation funct on (see (A-2) through (A-5)); however, the limitation $TW \gg 1$ must always hold. The multipath duration L can be made much larger than the inverse medium bandwidth W_m^{-1} by choosing the number of terms N in (6) large.

As a basis for comparison, the maximum possible value of deflection $d_e(t)$ is used. This is the value attained by a hypothetical receiver which knows the medium impulse response, in addition to the transmitted signal; also, the transmitter is presumed to have knowledge of the medium impulse response. The maximum possible value is given in (B-12) from appendix B:

$$d_{e_2} = \frac{E_x}{8N_d}\max_f\left|H_m(f)\right|^2. \tag{10}$$

The maximum is realized by concentrating the transmitted signal spectrum at the peak transmission frequency of the medium. The results to follow pertain to the ratios of deflection criteria

$$\frac{d_e(t)}{d_{e_2}} \quad \text{and} \quad \frac{d_r(t)}{d_{e_2}}. \tag{11}$$

Before we embark on the detailed numerical investigation of (11), some useful insight into good medium utilization can be obtained from (10). Suppose the medium transfer function is such that $|H_m(f)|^2$ is fairly flat in frequency; for example, suppose the peak-to-average ratio of $|H_m(f)|^2$ is of the order of 2. Then, since a significant change in $|H_m(f)|^2$ can occur in an interval of $1/L$ hertz, the transmitted signal will encounter the average transfer value if $W >> 1/L$, and values of (11) in the neighborhood of 1/2 can be anticipated. Thus a spread signal spectrum with $W > 1/L$ is a form of diversity which avoids encountering solely a deep fade in the medium. Values of (11) in the vicinity of 1/2 indicate good utilization of that particular medium, considering that the detailed impulse response is not known to the processor under investigation here. Of course, values of (11) much smaller than unity are realized when the medium transfer function has at least one frequency of large gain; however, this frequency would change with time and be unknown in most practical situations. Thus values of (11) much smaller than unity do not necessarily indicate a poor processor, but rather a medium that would require continuous measurement and characterization for optimum utilization.

The first impulse response considered consists of two positive pulses,* as indicated in figure 3A. Plots of the normalized deflections

$$\frac{d_e(t)}{\max_t d_e(t)} \quad \text{and} \quad \frac{d_r(t)}{\max_t d_r(t)} \tag{12}$$

are given in figures 3B and 3C, respectively, for $WL = 1.4$. The envelope detector output deflection in figure 3B is beginning to be resolved into two components; for larger values of W, two distinct pulses occur in $d_e(t)$. The ratios of deflection criteria, (11), are plotted in figures 3D and 3E, respectively, for WL in the range (0, 8). It is seen that the best value of signal bandwidth W for this impulse response (figure 3A) is zero. This is in agreement with (10), because the largest value of the medium transfer function occurs at $f = 0$. There is no point in resolving the multipath structure when the complex envelope of the medium impulse response has the same phase for all values of τ.

However, a slight change in center frequency, f_o, of the transmitted signal or the difference of medium paths delays, τ_d, can cause a significant phase shift of components of $h_m(\tau)$. For example, in appendix C, it is shown that a change in $f_o \tau_d$ of 1/2 causes the two pulses in figure 3A to have opposite

*Absolute levels are not important in the impulse response and therefore are not indicated.

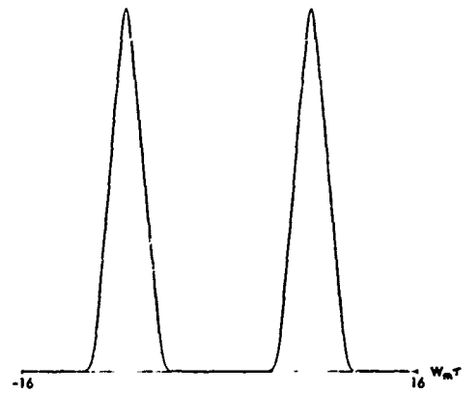

Figure 3A. Medium Impulse Response

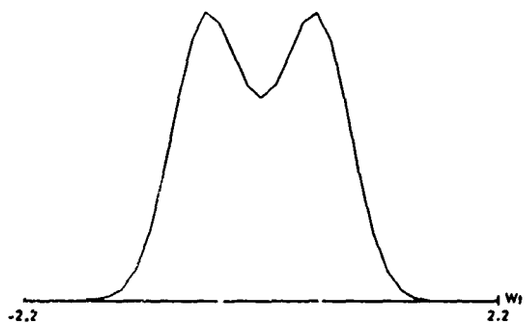

Figure 3B. Normalized Deflection $d_e(t)/\max_t d_e(t)$; WL = 1.4

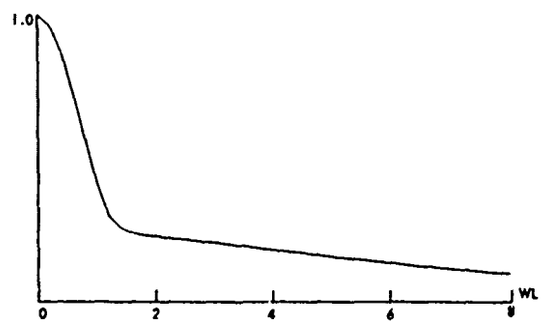

Figure 3D. Ratio of Deflection Criteria, $\max_t d_e(t)/d_{e_2}$

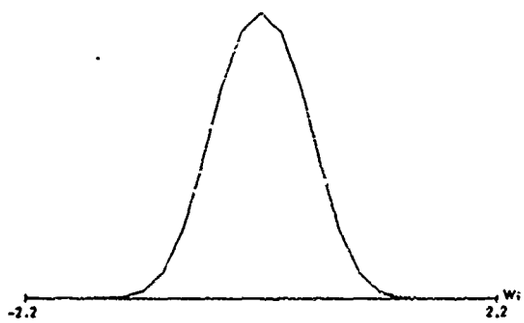

Figure 3C. Normalized Deflection $d_r(t)/\max_t d_r(t)$; WL = 1.4, $L_a/L = 1$

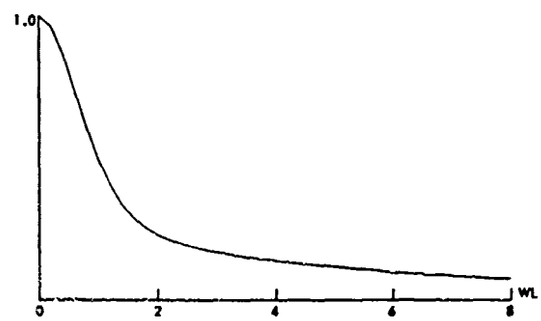

Figure 3E. Ratio of Deflection Criteria, $\max_t d_r(t)/d_{e_2}$; $L_a/L = 1$

Figure 3. System Performance for a Unipolar Impulse Response

polarities. This case is considered in figure 4A. The normalized deflections, (12), are plotted in figures 4B and 4C, respectively, for the case of WL = 1.6, where the two paths are well resolved. The ratios of deflection criteria, (11), are given in figures 4D and 4E. It is seen that best performance is attained for WL approximately equal to 1.6 for this example. If W is chosen too small, the two paths in figure 4A are not resolved and combine destructively. As W is increased, each path contributes separately (figure 4B), but if W is made too large, too much additional noise is allowed through receiver filter $h_r(\tau)$ in figure 1, and performance degrades, as indicated in figures 4D and 4E. The peak ordinates of 0.25 in figures 4D and 4E indicate rather good utilization of the medium; furthermore, the peak is fairly broad.

A third impulse response is indicated in figure 5A. It consists of two weak long-duration paths and two strong short-duration paths. The two normalized deflections, (12), are plotted in figures 5B and 5C, respectively, for WL = 2.0. The ratios of deflection criteria, (11), which are depicted in figures 5D and 5E, show that, as WL is increased from zero, the weak long-duration paths are resolved and performance improves. However, once these paths are resolved, additional bandwidth allows in more noise, and performance degrades. But if the bandwidth is increased still further, so as to resolve the strong short-duration paths, performance is again improved. However, sufficient bandwidth to attain this performance may not be available.

DISCUSSION

The performance of the system considered here depends on the precise details of the medium (complex envelope) impulse response, which has been modeled as a deterministic linear filter, unknown to the transmitter and receiver. Unless the medium is continuously measured and characterized, signal design ought to be accomplished for the "average" medium behavior rather than attempt to exploit some short-term behavior, with possible drastic fades and degradations in performance. For a medium with impulse duration L, the signaling bandwidth W should generally be taken larger than 1/L, the exact amount depending on the particular impulse response. For too large a value of W, the receiver-matched filter passes too much noise, which can not always be overcome through multipath resolution and incoherent combination. Also, interference limitations with other transmitters and receivers may preclude large signal bandwidths.

For $W < 1/L$, the medium acts like a single path with strength $\left|\int d\tau h_{in}(\tau)\right|$, which may be strong or weak, depending on the relative strengths and phases of component paths. That is, constructive or destructive addition can occur. This precarious situation can be alleviated by choosing $W > 1/L$; this is a form of diversity that makes drastic performance losses far less likely.

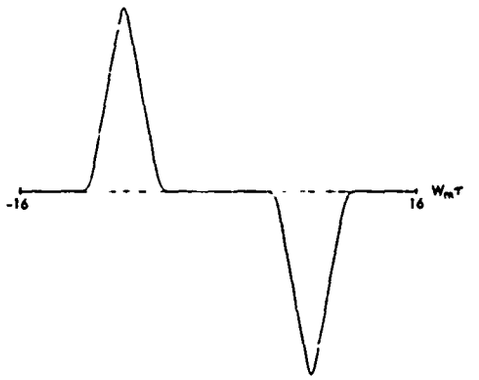

Figure 4A. Medium Impulse Response

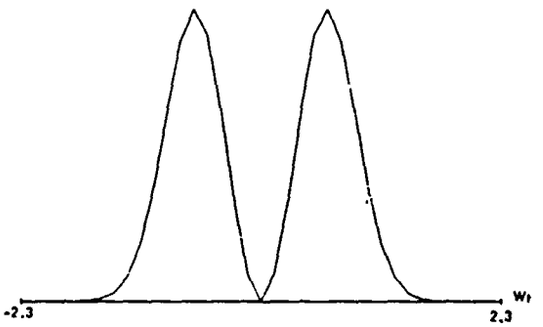

Figure 4B. Normalized Deflection $d_e(t)/\max_t d_e(t)$; WL = 1.6

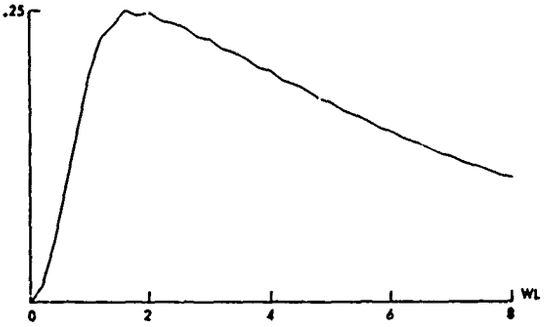

Figure 4D. Ratio of Deflection Criteria, $\max_t d_e(t)/d_{e_2}$

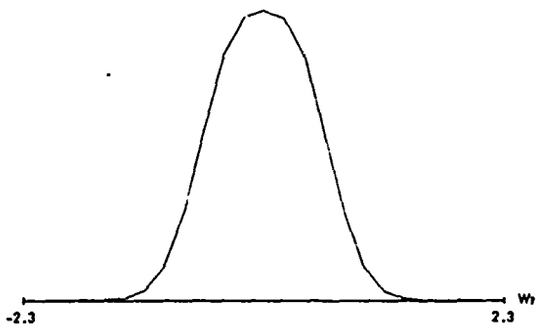

Figure 4C. Normalized Deflection $d_r(t)/\max_t d_r(t)$; WL = 1.6, $L_a/L = 1$

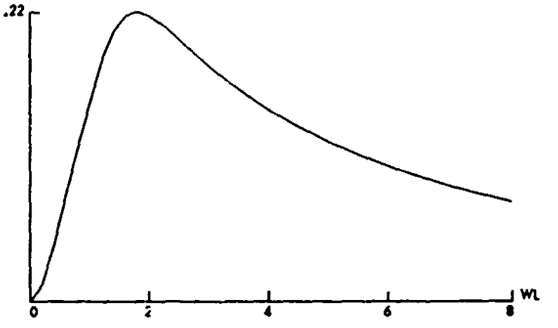

Figure 4E. Ratio of Deflection Criteria, $\max_t d_r(t)/d_{e_2}$; $L_a/L = 1$

Figure 4. System Performance for a Bipolar Impulse Response

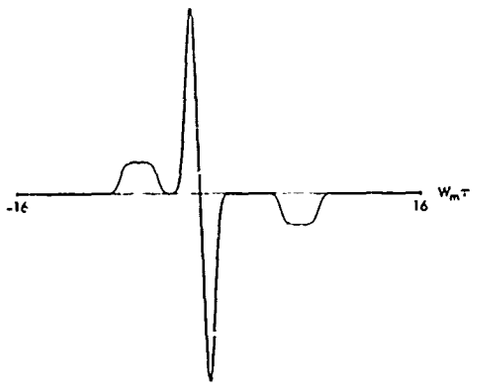

Figure 5A. Medium Impulse Response

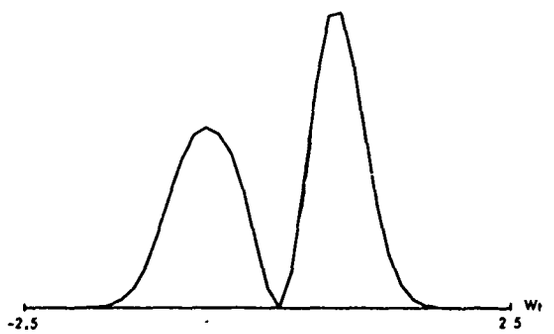

Figure 5B. Normalized Deflection $d_e(t)/\max_t d_e(t)$; WL = 2.0

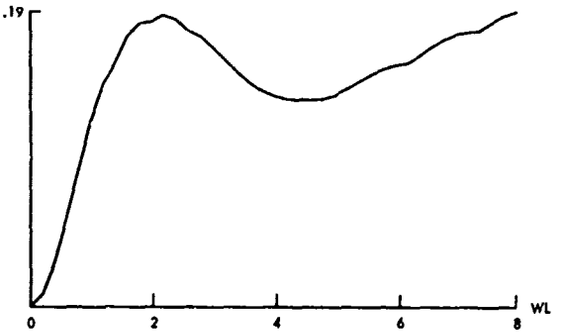

Figure 5D. Ratio of Deflection Criteria, $\max_t d_e(t)/d_{e_2}$

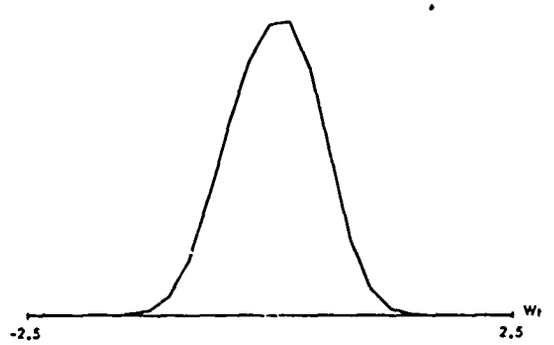

Figure 5C. Normalized Deflection $d_r(t)/\max_t d_r(t)$; WL = 2.0, L_a/L - 1

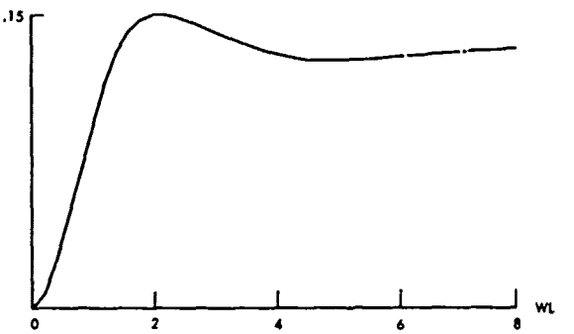

Figure 5E. Ratio of Deflection Criteria, $\max_t d_r(t)/d_{e_2}$; $L_a/L = 1$

Figure 5. System Performance for a Distributed Impulse Response

The incoherent combination of resolved outputs e(t) in figure 1 is accomplished by averaging filter $h_a(\tau)$, which was chosen here as a simple unimodal filter of duration approximately L. The results of figures 3E, 4E, and 5E indicate that the deflection values have not been increased above those before incoherent combination. The reason for this behavior is that the noisy intervals at the detector output have also been accumulated by the averaging filter, in addition to the signal contributions. If the envelope-detected output e(t) were subjected instead to a thresholding operation, and then passed through the averaging filter, the output deflection would be given approximately by

$$\frac{1}{\sqrt{M}} \sum_{k=1}^{M} d_e(t_k) , \tag{13}$$

where M is the number of threshold excursions, and $d_e(t_k)$ is the deflection criterion of the k-th excursion. For equal deflections, (13) increases proportionally with $\sqrt{M}$; thus incoherent combination can yield significantly better performance.

The main assumptions in this investigation are summarized below:

$$\begin{aligned} &TW \gg 1 , \\ &B^{-1} > T > L , \\ &\text{no Doppler} . \end{aligned} \tag{14}$$

Thus the medium must be under-spread, BL must be less than 1, and signal duration T must be appropriately chosen to fit the medium parameters. The conclusion drawn here for the real impulse responses in figures 3 through 5 apply equally well to complex impulse responses.

Appendix A

DERIVATION OF DEFLECTION CRITERIA

SIGNAL-ONLY OUTPUT

From figure 1 in the main text, recall that complex notation is utilized, and then

$$Y(f) = \tfrac{1}{2} H_m(f) X(f),$$

$$Z(f) = \tfrac{1}{2} H_r(f) Y(f) = \tfrac{1}{4} H_r(f) H_m(f) X(f),$$

$$z(t) = \tfrac{1}{4} h_m(t) \circledast \left[h_r(t) \circledast x(t) \right]. \tag{A-1}$$

The time function $h_r(t) \circledast x(t)$ measures the response of the receiver processing filter to the transmitted signal. If the receiver processing filter is matched to the transmitted signal, then, using (1) from the main text, we have

$$h_r(t) \circledast x(t) = x^*(-t) \circledast x(t) = \int d\tau\, x(\tau)\, x^*(\tau - t) = \phi(t), \tag{A-2}$$

where $\phi(t)$ is the autocorrelation of the signal $x(t)$. (For a Doppler shift, $\phi(t)$ would have to be replaced by the ambiguity function of signal $x(t)$.) Then (A-1) becomes

$$z(t) = \tfrac{1}{4} h_m(t) \circledast \phi(t), \tag{A-3}$$

where

$$\phi(0) = \int dt\, |x(t)|^2 = 2E_x. \tag{A-4}$$

Here E_x is the transmitted signal energy. A sample plot of $\phi(t)/\phi(o)$ is given in figure A-1.

The autocorrelation $\phi(t)$ is composed of two types of components, the single large peak of width $1/W$ and the small sidelobes; recall that $TW >> 1$. The convolution of the sidelobes of $\phi(t)$ with the details of $h_m(t)$ in (A-3) will not yield a significant contribution in comparison with that due to the main peak,

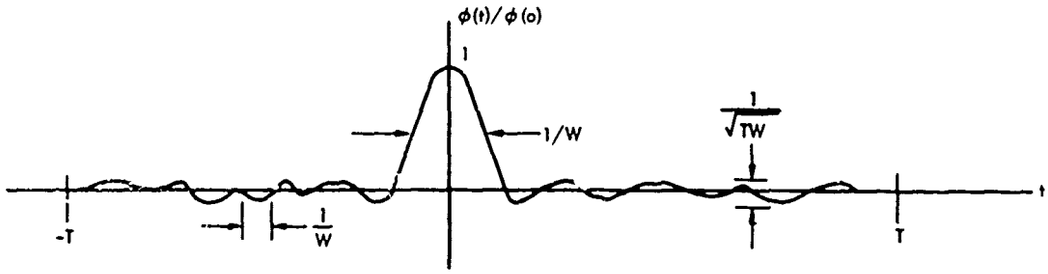

Figure A-1. Autocorrelation of Signal

since contributions from some positive sidelobes are cancelled by some from negative sidelobes. Hence the sidelobe contributions are ignored. (Actually this is a pessimistic assumption for signal detectability because these low-level components, after detection and low-pass filtering, constitute a broad increase in the average output above that normally due to the noise; see figure 2.)

In this case, we have, using (A-3), (A-4), and figure (A-1),

$$z(t) \cong \frac{1}{4} h_m(t) \circledast p(t), \tag{A-5}$$

where pulse p(t) is as shown in figure A-2.

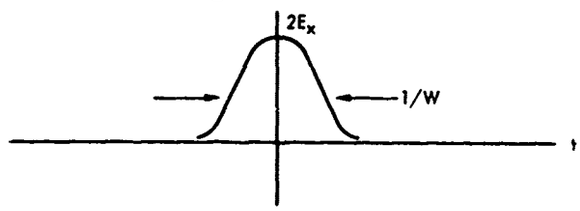

Figure A-2. Pulse Approximation to Autocorrelation

Then, using subscript s to denote the signal-only output, we have

$$e_s(t) = |z(t)|^2 = \frac{1}{16} \left| h_m(t) \circledast p(t) \right|^2, \tag{A-6}$$

and (no factor of 1/2 now because we use real waveforms instead of complex envelopes)

$$r_s(t) = h_a(t) \circledast e_s(t) = \frac{1}{16} h_a(t) \circledast \left| h_m(t) \circledast p(t) \right|^2. \tag{A-7}$$

Equations (A-6) and (A-7) are the main results for the signal-only output.

NOISE-ONLY OUTPUT

For noise only, $z(t)$ is a complex Gaussian process, with spectrum

$$G_z(f) = \tfrac{1}{4}\,|H_r(f)|^2\, G_n(f) = N_d\,|H_r(f)|^2, \tag{A-8}$$

where N_d is the double-sided spectrum level of the <u>real</u> received noise. Now

$$e(t) = |z(t)|^2. \tag{A-9}$$

The correlation function of $e(t)$ is (see reference 2)

$$\begin{aligned} R_e(\tau) &= \overline{e(t)\,e(t-\tau)} = \overline{|z(t)|^2 |z(t-\tau)|^2} \\ &= R_z^2(0) + |R_z(\tau)|^2. \end{aligned} \tag{A-10}$$

The spectrum of $e(t)$ is therefore

$$\begin{aligned} G_e(f) &= \int d\tau\, \exp(-i2\pi f\tau)\, R_e(\tau) \\ &= R_z^2(0)\,\delta(f) + G_z(f) \circledast G_z(f). \end{aligned} \tag{A-11}$$

The dc component of $e(t)$ does not hinder signal detection; it merely raises the bias level. The important quantity is the standard deviation of $e(t)$; thus consider

$$\begin{aligned} \mathrm{Var}\{e(t)\} &= \int df\,[G_z(f) \circledast G_z(f)] \\ &= \int df \int du\, G_z(f-u)\, G_z(u) = \left[\int df\, G_z(f)\right]^2 \\ &= \left[N_d \int df\, |H_r(f)|^2\right]^2. \end{aligned} \tag{A-12}$$

Therefore, using (2) and (A-4), we obtain

$$SD\{e(t)\} = N_d \int df\, |H_r(f)|^2 = N_d \int df\, |X(f)|^2 = N_d\, 2E_x. \tag{A-13}$$

This quantity is independent of the signal bandwidth W; the independence is due to the choice of receiver processing filter $H_r(f)$ as the matched filter to the transmitted signal.

The spectrum of the output r(t) is, using (A-11),

$$G_r(f) = |H_a(f)|^2 G_e(f)$$

$$= |H_a(f)|^2 \left[R_z^2(0)\delta(f) + G_z(f) \circledast G_z(f) \right]. \qquad \text{(A-14)}$$

The dc component in r(t) does not hinder signal detection. So we consider the

$$\text{Var}\{r(t)\} = \int df\, |H_a(f)|^2 \left[G_z(f) \circledast G_z(f) \right]$$

$$= N_d^2 \int df\, |H_a(f)|^2 \left[|H_r(f)|^2 \circledast |H_r(f)|^2 \right]$$

$$= N_d^2 \int df\, |H_a(f)|^2 \left[|X(f)|^2 \circledast |X(f)|^2 \right], \qquad \text{(A-15)}$$

upon using (A-8) and (3). This variance can depend on signal bandwidth W.

Putting on subscript n for noise alone, the main results for the noise-only output are

$$SD\{e_n(t)\} = 2E_x N_d, \qquad \text{(A-16)}$$

$$SD\{r_n(t)\} = N_d \left\{ \int df\, |H_a(f)|^2 \left[|X(f)|^2 \circledast |X(f)|^2 \right] \right\}^{1/2}. \qquad \text{(A-17)}$$

These two relations, combined with (A-6) and (A-7), afford evaluation of the deflection criteria in (4) and (5).

CHECK CASE

Consider $h_m(\tau)$ to be a broadband filter with unity <u>real</u> gain. Then $h_m(\tau)$ approaches $2\delta(\tau)$, a single-path medium. Now let $\tilde{z}(t)$ denote the real waveform corresponding to complex envelope z(t): $\tilde{z}(t) = \text{Re}\{z(t) \exp(i2\pi f_0 t)\}$. Then

$$\max_t \{\tilde{z}_s(t)\}^2 = \max_t \{|z_s^2(t)|\} = e_s(0)$$

$$= \frac{1}{16} |2p(0)|^2 = \frac{1}{16} 4(2E_x)^2 = E_x^2, \qquad \text{(A-18)}$$

using (A-6) and (A-4). This value could be realized only by a phase-coherent receiver. Also.

$$\text{Var}\left\{\tilde{z}_n(t)\right\} = E\left\{\tilde{z}_n^2(t)\right\} = \tfrac{1}{2} E\left\{|z_n(t)|^2\right\}$$

$$= \tfrac{1}{2}\int df\, G_z(f) = \tfrac{1}{2}\int df\, N_d |X(f)|^2 = N_d E_x, \tag{A-19}$$

using (A-8), (2), and (A-4). Therefore,

$$\left[\frac{\max_t\left\{\tilde{z}_s(t)\right\}}{SD\left\{\tilde{z}_n(t)\right\}}\right]^2 = \frac{E_x}{N_d}, \tag{A-20}$$

which is the standard result for a phase-coherent matched filter for a single-path in white noise, since E_x is also the received signal energy in this case. There also follows

$$\frac{\max_t\left\{e_s(t)\right\}}{SD\left\{e_n(t)\right\}} = \frac{\max_t\left\{|z_s(t)|^2\right\}}{SD\left\{|z_n(t)|^2\right\}} = \frac{E_x^2}{2N_d E_x} = \frac{1}{2}\frac{E_x}{N_d}. \tag{A-21}$$

The factor of 1/2 is due to the squared-envelope detector; the denominator is twice as large in this latter case (see (B-9) through (B-11)).

IMPULSE RESPONSE MODEL AND SIMPLIFYING APPROXIMATIONS

A general model of the medium impulse response $h_m(\tau)$ is afforded by a sum of spaced complex Gaussian pulses:

$$h_m(\tau) = W_m \sum_{k=-N}^{N} A_k \exp\left[-\pi\left(W_m\tau - \frac{3}{4}k\right)^2\right]. \tag{A-22}$$

The spacing of the component pulses is illustrated in figure A-3. The non-zero

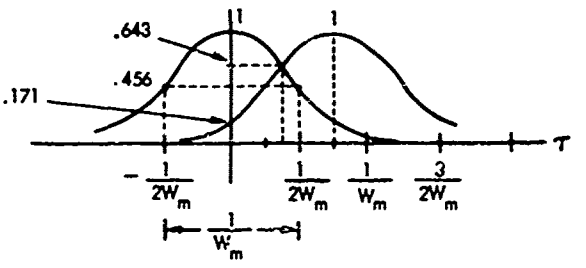

Figure A-3. Spacing and Overlap of Component Pulses

$\{A_k\}$ extend only over an interval covering L seconds, where (from A-22)),

$$L = \frac{1}{W_m}\left(1 + \frac{3}{2}N\right). \tag{A-23}$$

Medium impulse response $h_m(\tau)$ can change significantly every $1/W_m$ seconds; however, it does not have to, if several adjacent A_k are approximately equal. The medium transfer function is given by

$$H_m(f) = \exp\left(-\pi f^2/W_m^2\right) \sum_{K=-N}^{N} A_k \exp\left(-i2\pi \frac{f}{W_m} \frac{3}{4} K\right). \tag{A-24}$$

The signal autocorrelation pulse $p(t)$ in figure A-2 is represented as

$$p(t) = 2E_x \exp\left(-\pi W^2 t^2\right), \tag{A-25}$$

and is depicted in figure A-4. The energy density spectrum of signal $x(t)$ is

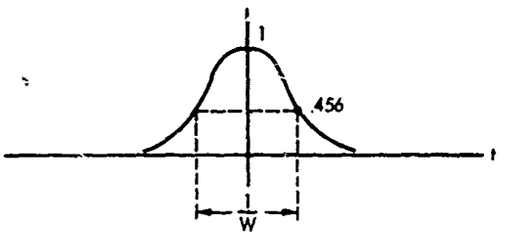

Figure A-4. Autocorrelation Pulse Shape

then given by

$$\begin{aligned} |X(f)|^2 &= \left|\int dt \exp(-i2\pi ft)\, x(t)\right|^2 \\ &= \int d\tau \exp(-i2\pi f\tau)\, \phi(\tau) \\ &\cong \int d\tau \exp(-i2\pi f\tau)\, p(\tau) \\ &= \frac{2E_x}{W} \exp\left(-\pi f^2/W^2\right), \end{aligned} \tag{A-26}$$

using (A-2), (A-25), and figures (A-1) and (A-2). Thus the approximation of signal correlation $\phi(\tau)$ by pulse $p(\tau)$ is tantamount to ignoring the detailed wiggles in the energy density spectrum $|X(f)|^2$, which are of width $1/T$, and considering $|X(f)|^2$ to be a broadband flat function with bandwidth W. This is a good approximation to energy density spectra of pseudorandom signals $x(t)$ with large TW product, for example.

The averaging filter $h_a(\tau)$ is represented by

$$h_a(\tau) = \frac{1}{L_a} \exp\left(-\pi \tau^2 / L_a^2\right),$$

$$H_a(f) = \exp\left(-\pi L_a^2 f^2\right), \tag{A-27}$$

and is indicated in figure (A-5).

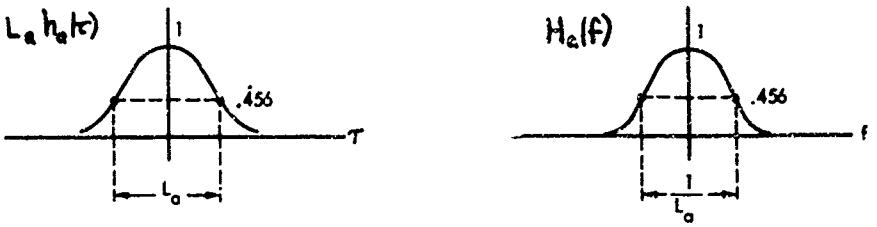

Figure A-5. Averaging Filter Characteristics

All necessary scale factors have been included in the medium, signal, and filter characteristics above. We now begin the evaluation of (A-6), (A-7), and (A-17). From (A-22) and (A-25),

$$h_m(t) \circledast p(t) = \frac{2E_x}{\sqrt{1+\frac{W^2}{W_m^2}}} \sum_{k=-N}^{N} A_k \exp\left[-\pi \frac{\left(Wt - \frac{3}{4}k\frac{W}{W_m}\right)^2}{1+\frac{W^2}{W_m^2}}\right]. \tag{A-28}$$

Then (A-6) yields

$$e_s(t) = \frac{1}{4} \frac{E_x^2}{1+\frac{W^2}{W_m^2}} \left| \sum_{k=-N}^{N} A_k \exp\left[-\pi \frac{\left(Wt - \frac{3}{4}k\frac{W}{W_m}\right)^2}{1+\frac{W^2}{W_m^2}}\right] \right|^2. \tag{A-29}$$

Substitution of (A-27) and (A-28) in (A-7) also yields

$$r_s(t) = \frac{E_x^2/4}{\left(1+\frac{W^2}{W_m^2}\right)^{1/2}\left(1+\frac{W^2}{W_m^2}\left(1+2L_a^2W_m^2\right)\right)^{1/2}} \sum_{k,\ell=-N}^{N} A_k A_\ell^* \cdot$$

$$\exp\left[-\frac{9}{32}\pi \frac{W^2/W_m^2}{1+W^2/W_m^2}(k-\ell)^2 - 2\pi \frac{\left(Wt - \frac{3}{8}(k+\ell)\frac{W}{W_m}\right)^2}{1+\frac{W^2}{W_m^2}\left(1+2L_a^2W_m^2\right)}\right]. \tag{A-30}$$

From (A-26), we find

$$|X(f)|^2 \circledast |X(f)|^2 = \frac{2\sqrt{2}E_x^2}{W} \exp\left(-\frac{\pi}{2}\frac{f^2}{W^2}\right). \tag{A-31}$$

Then employ (A-27) and obtain

$$\int df\, |H_a(f)|^2 \left[|X(f)|^2 \circledast |X(f)|^2 \right] = \frac{4E_x^2}{(1+4L_a^2W^2)^{1/2}} . \tag{A-32}$$

Substitution into (A-17) yields

$$SD\{r_n(t)\} = \frac{2E_x N_d}{(1+4L_a^2W^2)^{1/4}} . \tag{A-33}$$

The deflection criterion $d_e(t)$ in (4) follows from (A-29) and (A-16):

$$d_e(t) = \frac{E_x}{8N_d} \frac{1}{1+\frac{W^2}{W_m^2}} \left| \sum_{k=-N}^{N} A_k \exp\left[-\pi \frac{\left(Wt - \frac{3}{4}k\frac{W}{W_m}\right)^2}{1+\frac{W^2}{W_m^2}} \right] \right|^2 . \tag{A-34}$$

The deflection criterion $d_r(t)$ in (5) follows from (A-30) and (A-33):

$$d_r(t) = \frac{E_x}{8N_d} \left[\frac{\left(1+4L_a^2W_m^2\frac{W^2}{W_m^2}\right)^{1/2}}{\left(1+\frac{W^2}{W_m^2}\right)\left(1+\frac{W^2}{W_m^2}\left(1+2L_a^2W_m^2\right)\right)} \right]^{1/2} \cdot$$

$$\sum_{k,\ell=-N}^{N} A_k A_\ell^* \exp\left[-\frac{1}{32}\pi \frac{W^2/W_m^2}{1+W^2/W_m^2}(k-\ell)^2 - 2\pi \frac{\left(Wt - \frac{3}{8}(k+\ell)\frac{W}{W_m}\right)^2}{1+\frac{W^2}{W_m^2}\left(1+2L_a^2W_m^2\right)} \right] . \tag{A-35}$$

As a check on (A-34) and (A-35), let all the $A_k = 0$ except $A_0 = 2$, and let $W_m \gg W$. Then $h_m(\tau) \to 2\delta(\tau)$, and

$$d_e(0) = \frac{1}{2}\frac{E_x}{N_d} , \quad \dot{e}_r(0) = \frac{1}{2}\frac{E_x}{N_d} . \tag{A-36}$$

The first relation in (A-36) checks (A-21), as it should.

The fundamental parameters in (A-34) and (A-35) are N, $\{A_k\}_{-N}^{N}$, LW, and L_a/L. All other parameters depend on these:

$$\begin{aligned} LW_m &= 1 + \tfrac{3}{2}N \qquad \text{(from (A-23))}, \\ L_a W_m &= \frac{L_a}{L} LW_m \\ \frac{W}{W_m} &= \frac{LW}{LW_m} . \end{aligned} \tag{A-37}$$

Appendix B

PERFORMANCE OF THE OPTIMUM PROCESSOR

In the system of figure 1 in the main text, instead of choosing receiver filter $h_r(\tau)$ to be the matched filter to the transmitted signal $x(t)$, let us choose it as the filter that maximizes the signal-to-noise ratio at the filter output. This will require knowledge of the medium characteristics, and is therefore often not a practical alternative; however, it serves as a worthwhile standard with which to compare practical processors.

The peak value of the real signal output of $h_r(\tau)$ in figure 1 is

$$\max_t \tilde{z}_s(t) = \max_t |z_s(t)| = \max_t \left| \int df \exp(i2\pi ft) \tfrac{1}{4} X(f) H_m(f) H_r(f) \right|. \quad \text{(B-1)}$$

The variance of the real noise output of $h_r(\tau)$ is

$$\mathrm{Var}\left\{\tilde{z}_n(t)\right\} = \tfrac{1}{2} E\left\{|z_n(t)|^2\right\} = \tfrac{1}{2}\int df\, \mathcal{G}_{zz}(f) = \tfrac{1}{2} N_d \int df\, |H_r(f)|^2, \quad \text{(B-2)}$$

using the upper line of (A-19) and (A-8) from appendix A. The signal-to-noise ratio adopted at the output of $h_r(\tau)$ is

$$SNR = \frac{\left[\max_t \tilde{z}_s(t)\right]^2}{\mathrm{Var}\left\{\tilde{z}_n(t)\right\}} = \frac{1}{\frac{1}{2}N_d} \frac{\max_t \left| \int df \exp(i2\pi ft) X(f) H_m(f) H_r(f) \right|^2}{\int df\, |H_r(f)|^2}. \quad \text{(B-3)}$$

This quantity is maximized by the choice of receiving filter as

$$H_{r_1}(f) = H_m^*(f) X^*(f) \exp(-i2\pi f t_0), \quad \text{(B-4)}$$

where t_0 is the time at which the signal peak is desired. The maximum value of SNR is

$$SNR_1 = \frac{1}{\frac{1}{2}N_d} \int df\, |X(f)|^2 |H_m(f)|^2. \quad \text{(B-5)}$$

Now let us further maximize (B-5) by the choice of the transmitted signal x(t). Since

$$\int df\, |X(f)|^2 = 2E_x \quad \text{(B-6)}$$

from (A-4), the best signal energy density spectrum would be one concentrated at the frequency of maximum transfer of the medium.* The resulting signal-to-noise ratio is

$$SNR_2 = \frac{E_x}{4N_d} \max_f |H_m(f)|^2. \tag{B-7}$$

This is the ultimate value of signal-to-noise ratio attainable through design of both the transmitter and receiver, where both have knowledge of the medium characteristics.

For the ideal single-path medium with unity real gain, we have

$$h_m(\tau) = 2\delta(\tau), \quad H_m(f) = 2, \tag{B-8}$$

and (B-7) yields the standard value of E_x/N_d (see the check case in appendix A).

Since the envelope-squared detector in figure 1 is characterized by (3) from the main text, we observe that

$$\max_t e_s(t) = \max_t |z_s(t)|^2, \tag{B-9}$$

$$Var\{e_n(t)\} = E\{|z_n(t)|^4\} - E^2\{|z_n(t)|^2\} = E^2\{|z_n(t)|^2\}, \tag{B-10}$$

where we have utilized the fact that $z_n(t)$ is a Gaussian complex-envelope process (see reference 2). The peak of the deflection criterion at the envelope-detector output can be expressed in terms of SNR as

$$\max_t d_e(t) = \frac{\max_t e_s(t)}{SD\{e_n(t)\}} = \frac{\max_t |z_s(t)|^2}{E\{|z_n(t)|^2\}} = \frac{1}{2} SNR, \tag{B-11}$$

employing (B-1) through (B-3). For the optimum receiving filter of (B-4), (B-11) becomes

$$d_{e_2} = \frac{E_x}{8N_d} \max_f |H_m(f)|^2. \tag{B-12}$$

*This would require $1/T \ll 1/L$; i.e., signal duration T must be much larger than the multipath duration L.

This is the maximum possible value of $d_e(t)$ defined in (4) and is used as a standard for comparison with actual processors that are ignorant of the medium impulse response.

The following relations enable an illuminating conclusion about the behavior of (B-12). The medium transfer function satisfies

$$|H_m(f)|^2 = \left|\int d\tau \exp(-i2\pi f\tau)\, h_m(\tau)\right|^2$$

$$= \int du \exp(-i2\pi fu)\, \phi_m(u), \tag{B-13}$$

where $\phi_m(u)$ is the autocorrelation of the medium impulse response:

$$\phi_m(u) = \int d\tau\, h_m(\tau) h_m^*(\tau - u). \tag{B-14}$$

Now if $h_m(\tau)$ were, for example, a pseudorandom sequence of the numbers ± 1, then $\phi_m(u)$ would possess a single large peak at the origin, and small subsidiary peaks of different polarities and sizes elsewhere. Then $|H_m(f)|^2$, being a Fourier transform of $\phi_m(u)$, would consist of a number of peaks, each of approximately equal value, but would possess no dominant peak. For example, $|H_m(0)|^2 = |\int d\tau h_m(\tau)|^2$, which is much smaller than $[\int d\tau |h_m(\tau)|]^2$ for this pseudorandom example; this latter quantity is obtainable for a medium with like-polarity peaks. Therefore, (B-12) for the optimum processor would not be expected to be much larger than deflection criteria (A-34) and (A-35), for this particular realization of the medium. More generally, if $h_m(\tau)$ has no pronounced periodic behavior in τ, and if it has values of both polarities (actually complex values generally), then (B-12) is expected to be fairly closely attained by the suboptimum processor investigated here. This follows if the signal bandwidth W can be made large enough to resolve all the individual multipaths; this may not be possible in a practical situation.

Appendix C

PHASE SHIFT OF THE COMPLEX-ENVELOPE IMPULSE RESPONSE

Consider a medium with real impulse response

$$\tilde{h}_m(\tau) = \tilde{a}(\tau) + \tilde{a}(\tau - \tau_d), \tag{C-1}$$

where τ_d is the difference in delay between two paths, each with identical response $\tilde{a}(\tau)$. Then the real transfer function is

$$\tilde{H}_m(f) = \tilde{A}(f)\left[1 + \exp(-i2\pi f \tau_d)\right], \tag{C-2}$$

and the complex-envelope transfer function is

$$\begin{aligned} H_m(f) &= 2U(f+f_o)\tilde{H}_m(f+f_o) \\ &= 2U(f+f_o)\tilde{A}(f+f_o)\left[1 + \exp(-i2\pi(f+f_o)\tau_d)\right] \\ &= A(f)\left[1 + \exp(-i2\pi(f+f_o)\tau_d)\right], \end{aligned} \tag{C-3}$$

where f_o is the signal center frequency, and $U(f) = 0$ for $f < 0$, 1 for $f > 0$. The complex envelope impulse response follows as

$$h_m(\tau) = a(\tau) + a(\tau - \tau_d)\exp(-i2\pi f_o \tau_d). \tag{C-4}$$

Now if $f_o \tau_d$ is an integer, the exponential in (C-4) is +1. However, if $f_o \tau_d$ is a half-integer, the exponential is -1. Therefore a change in $f_o \tau_d$ as small as 1/2 can cause a phase reversal in component pulses of the complex impulse response; this holds regardless of the polarity or complexity of component responses $a(\tau)$.

LIST OF REFERENCES

1. A. H. Nuttall and D. W. Hyde, Operating Characteristics for Continuous Square-Law Detection in Gaussian Noise, NUSC Technical Report 4233, 3 April 1972.

2. A. H. Nuttall, "High-Order Covariance Functions for Complex Gaussian Processes," IEEE Transactions on Information Theory, vol. IT-8, no. 3, April 1962, pp. 255-256.

REVERSE BLANK